

Development of Non-ferrous Superconducting Magnets

Frank Krienen, Dinesh Loomba, Wuzheng Meng
 Dept. of Physics, Boston University
 10 November 1990

Abstract

The study deals with non-ferrous two-dimensional arrays of line currents, creating magnetic fields suitable for guiding or focusing particle beams. Complex potential theory is used throughout. Methods have been found to reduce stray fields which are lower than those of the ferromagnetic equivalents. Harmonic analysis shows that the quality of the useful field is on a par with the state of the art. In addition to cartesian coordinates, the potential theory is extended to elliptic coordinates. This provides greater freedom in shaping the aspect ratio of the useful field. Treated in detail is the proposed inflector for the muon g-2 experiment at BNL. A combined function magnet is developed, scaled to the CERN alternating gradient proton synchrotron. The principle of a dual beam facility has been advanced.

I. INTRODUCTION

Non-ferrous superconducting magnets feature superior linearity, allowing a larger dynamic range when these magnets are part of a particle accelerator, consisting of a lattice predominantly of dipoles and quadrupoles, and occasionally of higher order multipoles. The stability of the classical ferro-magnets is only apparent and applies to devices where the required precision is to the order of 100 ppm. Provided that the iron is not too much in saturation, the field shape in the gap is largely determined by the pole profile and the field precision is more or less tied to the stability of the current source. However, the magnet iron fails on the 1 ppm level, because of saturation, hysteresis, eddy currents, temperature or non-uniformity in the steel, so that the strength of the harmonics change relative to the strength of the dipole, when the current in the lattice is ramped up. Only in the case of fixed field magnets could one hope for higher accuracy [1].

The stray field of non-ferrous magnets can be a problem. However, it will be shown that current distributions can be found, so that the stray field is considerably lower than the stray field of an equivalent ferro-magnet. Magnetic sources external to non-ferrous magnets can also be a problem. In this case thin high permeability shields, surrounding the device will solve this.

II. CURRENT DISTRIBUTIONS

The magnetic elements of an accelerator lattice are essentially two-dimensional, this permits to apply complex potential theory, in which all potentials and field quantities are functions of $z = x + iy$.

a) *Generating currents on a circle.*

A surface current distribution on a circular cylinder of radius R may be written in its most general form:

$$K = \sum K_N = \sum [C_N \cos(N\theta) + S_N \sin(N\theta)] \quad (1)$$

θ is the polar angle, N=1 creates a dipole, N=2 a quadrupole, and so on. The amplitudes C_N and S_N determine the symmetry axes of the Nth component. We introduce the complex surface current amplitude κ :

$$\kappa_N = C_N - iS_N; \quad \bar{\kappa}_N = C_N + iS_N \quad (2)$$

through which the complex potential $\zeta = A - iG$, inside or outside the boundary, may be expressed in concise form:

$$\zeta^i = \sum \zeta_N^i = \sum \frac{\mu_0}{2N} \kappa_N \frac{z^N}{R^{(N-1)}} \quad |z| < R \quad (3)$$

$$\zeta^e = \sum \zeta_N^e = \sum \frac{\mu_0}{2N} \bar{\kappa}_N \frac{R^{(N+1)}}{z^N} \quad |z| > R \quad (4)$$

$R_e(\zeta) = A$, is the axial and only component of the vector potential \vec{A} , which determines the magnetic field: $\vec{B} = \text{curl} \vec{A}$. $I_m(\zeta) = -G$ determines, through its derivatives $\delta/\delta s$ on any boundary s, the surface current on that boundary:

$$\mu_0 K = \frac{\delta G^e}{\delta s} - \frac{\delta G^i}{\delta s} = \frac{\delta(G^e - G^i)}{\delta s} \quad (5)$$

b) *Generating currents on an ellipse*

Assuming that the two focal points are at $x = \pm c$, the family of confocal elliptic cylinders and the family of confocal hyperbolic cylinders, in elliptic coordinates, are

$$\frac{x^2}{\cosh^2 u} + \frac{y^2}{\sinh^2 u} = c^2 \quad (6)$$

$$\frac{x^2}{\cos^2 v} - \frac{y^2}{\sin^2 v} = c^2 \quad (7)$$

The complex spatial variable $w = u + iv$ will be defined by $\xi = \cosh(u)$, and $\eta = \cos(v)$. Lines of constant u are the confocal ellipses and lines of constant v are the confocal hyperbolae. The relation between z and w is now:

$$\frac{z}{c} = \cosh(w) \quad (8)$$

Thus eq.(8) is the complex potential of a dipole in relative units. Likewise, a multipole would assume the form $[\cosh(w)]^N$. The first 2 harmonics, in relative units, inside and outside the surface current boundary $u' = \text{constant}$, are now shown:

$$\zeta_1^i = \frac{z}{c} = \cosh(w)$$

$$\zeta_2^i = \left(\frac{z}{c}\right)^2 = \frac{1}{2} \cosh(2w) + \frac{1}{2} \quad u < u' \quad (9)$$

$$\zeta_1^c = e^{u'} \cosh(u') e^{-w}$$

$$\zeta_2^c = \frac{1}{2} e^{2u'} \cosh(2u') e^{-2w} + \frac{1}{2} \quad u > u' \quad (10)$$

The surface currents on the boundary, generating the above potentials are calculated according to eq.(5)[2].

c) *Distributions on two concentric circles, or on two confocal ellipses*

The complex potential produced by two concentric cosine theta distributions comprises three regions:

$$\zeta_1 = -\frac{\mu_0 K R}{2} \frac{z}{R} - \frac{\mu_0 K' R'}{2} \frac{z}{R'} \quad |z| < R$$

$$\zeta_2 = -\frac{\mu_0 K R}{2} \frac{R}{z} - \frac{\mu_0 K' R'}{2} \frac{R'}{z} \quad R < |z| < R'$$

$$\zeta_3 = -\frac{\mu_0 K R R}{2} \frac{R}{z} - \frac{\mu_0 K' R' R'}{2} \frac{R'}{z} \quad |z| > R' \quad (11)$$

A useful application of the double cosine theta distribution is treated in ref.[3]. A similar relation may be obtained for a pair of ellipses; this is treated in Section V.

d) *Truncation on a flux line*

One may modify the shape of the useful field volume if circles or ellipses, on which the surface current is projected, do not satisfy the needs. In this case, one uses only a part of the field region, i.e., the field is truncated. The truncation is invariably along a line of constant A . Only then is a surface current distribution able to nullify the field on the outside and to leave the inside field unchanged. The amount of current needed to achieve this, is given by the G-function, through eq.(5).

III. LINE CURRENTS

Assuming that the superconductors have a relatively small superconducting core, embedded in a larger stabilizing matrix, the continuous surface current must be concentrated in what one could call a distribution of line currents I . The sum of the total fluctuation[4], ΔG , in each branch is related to the number of turns in the same branch, n , as follows:

$$\sum \Delta G = n \mu_0 I \quad (12)$$

The method of positioning the wires consists of constructing an arithmetic series of G , so that:

$$G_{j+1} - G_j = \mu_0 I \quad (13)$$

One may now solve for the position z_j of the wire, as both A and G are known in the case of a truncation, or one coordinate plus G in the case of a circle or ellipse.

Having replaced the surface current distribution by a multi-wire system, one can investigate the influence of field quality due to the granularity, study the stray field and its interactions with the harmonic components of the external field[2].

IV. INFLECTOR

The inflection of a particle beam into a storage ring is usually done with a pulsed magnetic inflector. The persistence of the decaying eddy currents in this case can be troublesome for an ultra high precision measurement of the muon g-2 value in an experiment currently under design at the Brookhaven National Laboratory[5]. A superconducting dc septum magnet may overcome this problem, although the stray field is not less, per se, but allows at least static shimming and precise measurement of the numerical correction to be applied. We desire a useful channel area 45 mm high and 18 mm wide, with the dipole field strength of 15 kilogauss. Two variants are shown:

a) *The truncated double cosine theta septum*

According to eq.(11), truncation on a flux line and discretization into line currents yield a truncated double cosine theta septum[3][2]. Figure 1 is a flux plot generated by the POISSON Group Codes[6]. The contribution of K'_1 here is to squeeze the return flux. Three harmonic expansions of the field around two strategic centers are shown in [2].

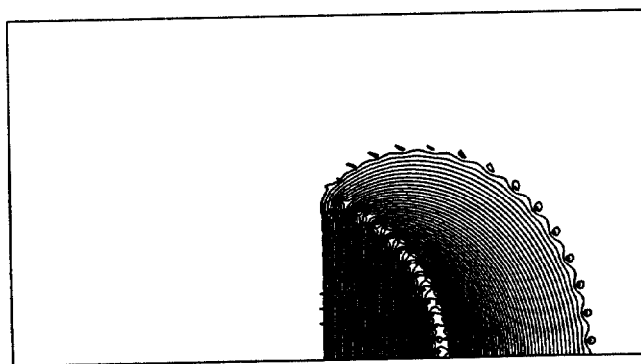


Figure 1: Flux plot of the inflector

b) *The truncated cosine theta distribution on which is superimposed a coaxial distribution*

By introduction of a term C_0 , may give an alternative solution to the squeezing of the return flux. The development of the "coaxial" inflector is described in [2]. It

Table 1: Parameters of Combined Function Configuration

a'	b'	c	a''	b''
2	1	$\sqrt{3}$	$2\sqrt{3}$	3
u	u''	d	q	λ
.5493	1.317	.2679	.0513	.2236

appears that there is a small savings in total number of ampere turns.

V. COMBINED FUNCTION

The excellent linearity of non-ferrous superconducting magnets may favor the come-back of the combined function configuration. The 25 GeV alternating gradient proton synchrotron at CERN [7] is taken as an example. The field of this magnet is a superposition of a dipole and a quadrupole. We develop such a system with the generating elements located on an ellipse, $u = u'$. In order to nullify the stray field at a certain distance, we add a similar pair of opposing fields having their generating elements on the confocal ellipse, $u = u''$, $u'' > u'$.

From eqs.(9)(10), potentials are calculated[2]. The parameters, in relative units, are summarized in Table 1, where a', b' and a'', b'' are the half axes of the ellipse $u = u'$ and $u = u''$, respectively; c is the focal length; d and q are the relative strength of the dipole, respectively quadrupole, generated on the outer ellipse; λ expresses the relative strength of quadrupole vs dipole and is thus of relevance for the focusing strength of the system, usually expressed through the n-value: $n = -(r_o/B_o)(dB/dr)$, or $\lambda = (n/r_o)[c(1-d)/(1-q)]$. The currents generating these fields are derived from the G-functions, using eq.(5)(13)[2]. Figure 2 shows a flux plot of the line currents.

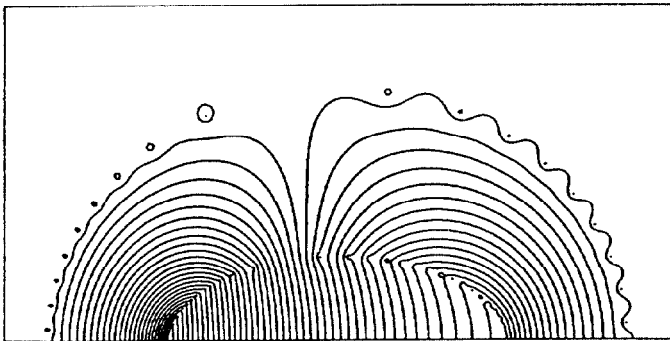


Figure 2: Flux plot of combined function distribution

VI. DUAL BEAM FACILITY

It may be possible to construct a magnet system suitable for the containment and the acceleration of dual particle

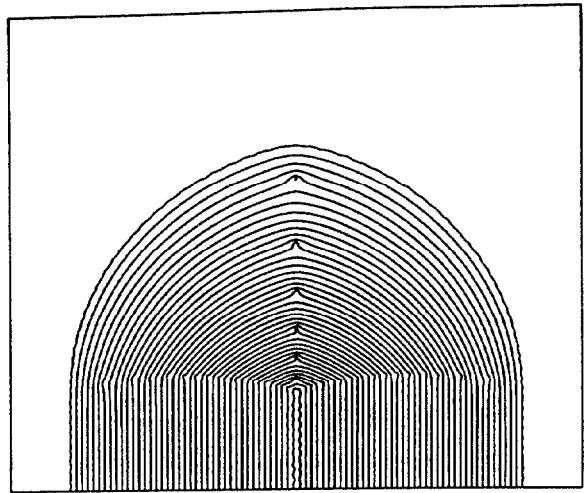


Figure 3: Flux plot of the dual beam facility

beams. These beams move in opposite direction, so that a colliding beam facility could be envisaged. We chose here elliptic coordinates in order to have more freedom in the aspect ratio of the channel. We superimpose a "coaxial" current distribution on the desired dipole current, modifying the field outside the ellipse only. The effect is to swing the outer flux to the right or the left, determined by the sign of the "coaxial" current. Truncating two such ellipses, with opposite dipole currents, one can obtain a dual dipole channel by "gluing" their return fluxes, provided the tangential mismatch is corrected at the interface. This is shown in Figure 3, in which the surface currents are discretized into line currents.

VIII. REFERENCES

- [1] H.Drumm et al. "The storage ring magnet of the third muon g-2 experiment at CERN", NIM vol.158, no.2-3, 15 Jan.1979, p.347-62.
- [2] F.Krienen et al. "Development of Non-ferrous Superconducting Magnets", Muon g-2 Note No.63, AGS, BNL, Nov.1990.
- [3] F.Krienen et al. "The truncated double cosine theta superconducting magnet", NIM A283(1989)5-12.
- [4] E.T.Whittaker & G.N.Watson, "A Course of Modern Analysis".
- [5] AGS Proposal 821, Sept.1985, revised Sept.1986, "A new precision measurement of the muon g-2 value at the level of 0.35 ppm."
- [6] J.Warren, et al. "POISSON/SUPERFISH Reference Manual", Los Alamos National Laboratory report LA-UR-87-126(January 1987)
- [7] C.A.Ramm et al. Considérations sur l'électro-aimant d'un synchrotron à gradient alterné. CERN Symposium 1956. Geneva, June 1956, Vol1, p307.